

Magnetic structure of erbium

Doon Gibbs, Jakob Bohr,* and J. D. Axe

Brookhaven National Laboratory, Upton, New York 11973

D. E. Moncton and K. L. D'Amico

Brookhaven National Laboratory, Upton, New York 11973

and Exxon Research and Engineering Company, Annandale, New Jersey 08801

(Received 23 May 1986; revised manuscript received 30 September 1986)

We present a synchrotron x-ray scattering study of the magnetic phases of erbium. In addition to the magnetic scattering located at the fundamental wave vector τ_m we also observe scattering from magnetoelastically induced charge modulations at the fundamental wave vector, at twice the fundamental, and at positions split symmetrically about the fundamental. As the temperature is lowered below 52 K the charge and magnetic scattering display a sequence of lock-in transitions to rational wave vectors. A spin-slip description of the magnetic structure is presented which explains the wave vectors of the additional charge scattering.

The competition among indirect-exchange, crystal-field, and magnetoelastic energies in the rare-earth metals is reflected in the variety of spiral, conical, c -axis-modulated, and ferromagnetic phases they display. Qualitatively, isotropic long-range, and competing exchange interactions among localized f electrons give rise to long-period magnetic modulation, while anisotropic crystal-field and magnetoelastic interactions distort these structures and may induce lock-in transitions to commensurate phases.¹ Recently, the results of synchrotron-based magnetic x-ray scattering experiments on holmium have led to a model of its magnetic structure containing spin defects originating in the competition between exchange and lattice interactions.^{2,3} An important feature of the x-ray results was the observation of an additional peak in the diffraction pattern arising from lattice modulations. It was shown that the additional scattering is due to correlation among the spin defects (which we call spin slips) present in holmium's magnetic spiral. The sensitivity of x rays to lattice modulations and the high resolution available from synchrotron radiation have thereby provided a powerful probe of the detailed structure of magnetic materials.

In this paper we present a high-resolution x-ray scattering study of the magnetic structure of erbium. From earlier neutron scattering⁴⁻⁶ studies it is known that over a wide temperature range erbium possesses a c -axis-modulated moment in addition to its basal plane or spiral component. The phase diagram is structurally complex and displays a variety of phases of which at least two are commensurate. Analysis⁷ of neutron scattering and magnetization data including effective crystal-field and interplanar exchange parameters has provided a semiquantitative description of the temperature and field dependence of the magnetic structure. Based on a mean-field calculation of the 3D Ising model with competing exchange interactions, a soliton description (similar to our spin-slip description) of pure c -axis magnetic structures has been suggested with a sequence of commensurate, incommensurate, and chaotic states.⁸ Here we will emphasize the additional role of magnetoelastic interactions. It is well known that

these terms give rise to *macroscopic* strains. More generally, they give rise to finite-wave-vector distortions of the charge density as have been observed at $2\tau_m$ in holmium⁹ and chromium.¹⁰ In the present research, a complex of lattice modulations is observed and their analysis leads to a natural description of the magnetic structure using the spin-slip model.

Erbium has an hcp crystal structure with two layers per chemical unit cell and a magnetic moment of about $9\mu_B/\text{atom}$. Neutron scattering studies have identified three distinct regions of magnetic order.⁴⁻⁶ Below the Néel temperature $T_N \approx 84$ K and above 52 K the moments are ordered parallel to the c axis and modulated with a slowly varying wavelength of approximately seven atomic layers. Near T_N only the fundamental magnetic reflections are observed, consistent with a simple sinusoidal modulation of the c -axis moment. Below 70 K weak third- and fifth-order harmonics appear, in addition to the primary satellite, indicating distortions of the purely sinusoidal order. For temperatures between 52 and 18 K an additional component of the spin develops in the basal plane forming a spiral modulation of identical period. As the temperature is lowered to ≈ 22 K additional odd harmonics of order up to 17 have been observed, suggesting a "squared-up" alternating cone structure.⁴ The temperature dependence of the modulation wave vector shows an inflection point near $\tau_m = \frac{4}{15}$ at 33 K and a lock-in transition to $\tau_m = \frac{1}{4}$ at 24 K.^{5,6} Below 18 K τ_m locks to a value $0.238 \approx \frac{5}{21}$ and erbium is believed to have a conical magnetic structure in which the c -axis component is ferromagnetic.⁵

For the synchrotron experiments an erbium single crystal ($9 \times 4 \times 3$ mm³) grown at Ames Laboratory was mounted in a variable-temperature cryostat and studied in the reflection geometry. Initial experiments, including polarization analysis, were carried out on the eight-pole wiggler beam line (VII-2) at the Stanford Synchrotron Radiation Laboratory (SSRL) using a Ge(111) double-crystal monochromator ($\lambda = 1.58$ Å) and Ge(111) analyzer. Subsequent experiments were performed at Brookhaven's Na-

tional Synchrotron Light Source (NSLS) using a bending-magnet beam line (22B) with a horizontal single-reflection Ge(111) monochromator ($\lambda = 1.7 \text{ \AA}$) and Ge(111) analyzer. At both beam lines the resolution full width at half maximum (FWHM) of the Er(002) reflection was about 0.0015 \AA^{-1} . Distinguishing magnetic and charge scattering in the x-ray experiments was accomplished by means of a polarization analyzer which has been described in detail elsewhere.¹¹ Neutron scattering experiments were performed on the cold-source triple-axis spectrometer at Brookhaven's High Flux Beam Reactor. Resolution of about 0.008 \AA^{-1} was achieved with a graphite (002) double-crystal monochromator ($\lambda = 4.05 \text{ \AA}$), a graphite (002) analyzer, and typical collimation.

Figure 1 summarizes the temperature dependence of the fundamental modulation wave vector τ_m and of the additional scattering observed at $2\tau_m$, τ_s , and $2\tau_m - \tau_s$. The figure combines synchrotron x-ray scattering results with neutron scattering results obtained on the same sample. Figure 2 displays the x-ray results for scattering at $2\tau_m$ on an expanded scale. All of the data presented here were

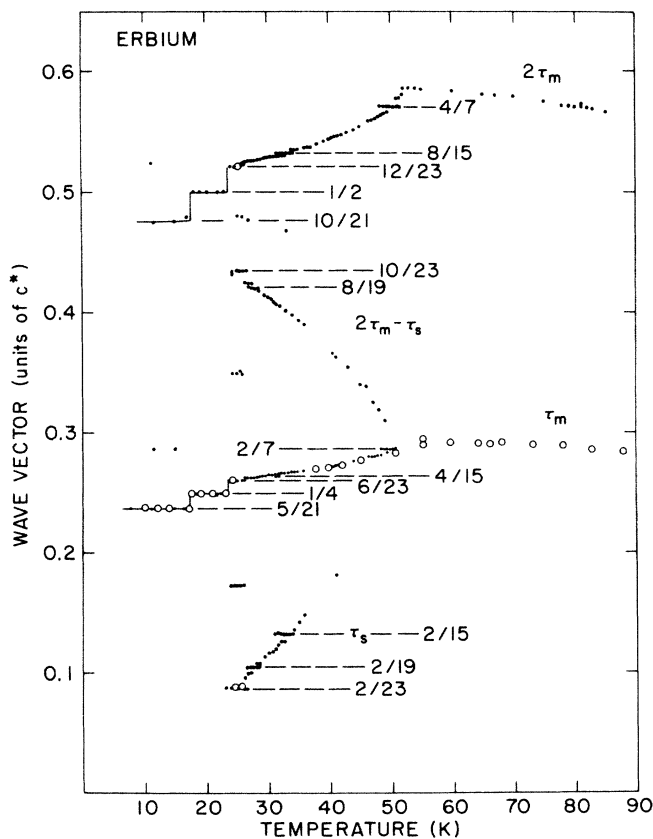


FIG. 1. Combined x-ray (●) and neutron scattering (○) results for the fundamental wave vector τ_m and for the additional scattering from lattice modulations at $2\tau_m$, τ_s , and $2\tau_m - \tau_s$. The peak observed at τ_m in the c -axis modulated phase above 52 K is the principle magnetic satellite of the (110) reflection, obtained by neutron scattering. All remaining data are satellites of the Bragg (002) and (004) reflections. The x-ray results at $2\tau_m - \tau_s = \frac{6}{15}$ were partially obscured by higher-order contamination.

taken for decreasing temperatures so that the data are free of hysteresis effects.

In the c -axis-modulated phase between 85 and 52 K scattering at τ_m (neutron) and $2\tau_m$ (x ray) is observed (Fig. 1). As the temperature is reduced the wave vector increases from $2\tau_m = 0.567$ at 85 K to a maximum near $2\tau_m = 0.587$ at 52 K (Fig. 2). Within this range the peak widths are resolution limited. At 52 K the basal-plane moments order and regions of the crystal are locked to $2\tau_m = \frac{4}{7} \approx 0.571$. Figure 3 shows the temperature dependence of the scattering near $2\tau_m$ for the $\tau_m = \frac{2}{7}$ transition. The peak at $\frac{4}{7}$ has a resolution-limited width while the coexisting peaks above and below $\frac{4}{7}$ are broader than resolution. Between 52 and 23 K x-ray scattering peaks appear at τ_m , τ_s , and at $2\tau_m - \tau_s$ (Fig. 1). As the temperature is reduced from 52 K the scattering at τ_m , $2\tau_m$, τ_s , and $2\tau_m - \tau_s$ exhibits a sequence of first-order transitions to rational wave vectors. In Fig. 2, for example, $2\tau_m$ successively locks to $\frac{4}{7}$, $\frac{8}{15}$, $\frac{12}{23}$, $\frac{1}{2}$, and $\frac{10}{21}$; near $2\tau_m = \frac{6}{11}$ and $2\tau_m = \frac{10}{19}$ the peak widths are observed to narrow. Further, when τ_m locks to $\frac{4}{15}$, $\frac{5}{19}$, and $\frac{6}{23}$ then τ_s locks to $\frac{2}{15}$, $\frac{2}{19}$, and $\frac{2}{23}$, respectively. These results are collected in Table I. Above 26.5 K the commensurate phases are separated by incommensurate phases whose peak widths are broader than the commensurate peak widths,¹² while below 26.5 K only commensurate phases occur. Between 26.5 and 23 K the peak intensities at $\tau_m = \frac{6}{23}$ and at $\tau_s = \frac{2}{23}$ increase by nearly a factor of 5, and harmonics develop at $\frac{4}{23}$, $\frac{8}{23}$, and at $\frac{11}{23}$ (Fig. 1). Below 18 K large signals are observed at the fundamental $\tau_m = \frac{5}{21}$ and weak, additional scattering is observed at $2\tau_m = \frac{10}{21}$ and at $\tau_s' = \frac{2}{7}$ (Figs. 1 and 2).

Using a polarization analyzer for distinguishing charge and magnetic scattering¹¹ we have verified that the peaks at $2\tau_m$ and at τ_s at 26 K result from charge scattering, due to lattice modulations, while the scattering at τ_m has both a charge and a magnetic component. We note that weak scattering at $2\tau_m$ and τ_s (in addition to the magnetic scattering at τ_m) has also been obtained by neutron dif-

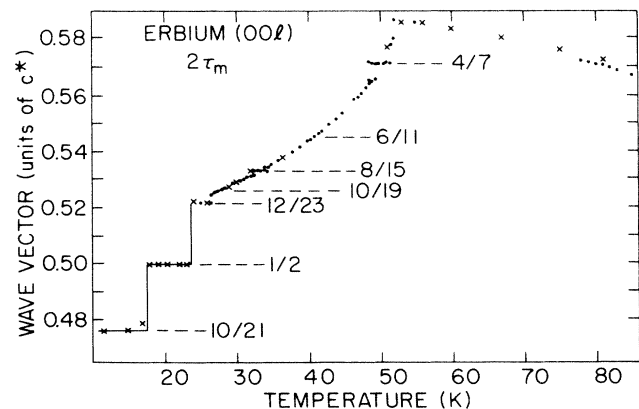


FIG. 2. Temperature dependence of twice the modulation wave vector $2\tau_m$ obtained by synchrotron x-ray scattering. ●'s were obtained at the NSLS while ×'s were obtained at the SSRL. The discrepancies in temperature above 50 K are the result of different thermometry used in the two experiments.

fraction at temperatures where the modulation is particularly strong (see open circles Fig. 1).

The magnetic and charge scattering observed in erbium may be understood using the concept of localized spin defects (spin slips) developed in earlier studies of holmium.^{2,3} Consider first the *c*-axis component of the modulation. The basic structural unit consists of four adjacent basal plane layers (a quartet) with identically aligned spins either parallel or antiparallel to the *c* axis. A single spin slip is created by associating one less spin to any quartet to form a triplet. For example, a structure with $\tau_m = \frac{2}{7}$ has an alternating sequence of quartets parallel and triplets

antiparallel. Generally, the modulation wave vector for a commensurate magnetic structure is the ratio of the number of full 2π rotations of the moments to the number of layers in the magnetic unit cell. Thus, the *c*-axis modulation has $\tau_m = 2n/(8n - s)$ in units of c^* , where n is the number of 2π rotations and s is the number of triplets. (The factor 2 enters because an hcp structure has two layers per chemical unit cell.)

The spin-slip structures generated in this way for the rational wave vectors observed in the data are shown in Table I in order of decreasing temperature. We adopt the notation $\cdot p$ in which a triplet is represented by \cdot and the integer p gives the number of quartets. In this notation $\cdot 1$ represents the slip structure with $\tau_m = \frac{2}{7}$.

The scattering at $2\tau_m$ may be understood by noting that the average number of layers between spins parallel or antiparallel to the *c* axis corresponds to one-half the magnetic period. Therefore, $2\tau_m$ defines the frequency of the accompanying magnetoelastic distortions.¹³ The lattice modulations measured by the scattering at τ_s and at $2\tau_m - \tau_s$ arise from correlations among the triplet and quartet distributions, respectively. For commensurate spin-slip structures we may calculate the wave vectors expected for charge scattering from the triplet, and quartet distributions as the ratio of the number of triplets and quartets, respectively, to the number of layers in the magnetic unit cell. Explicitly, $\tau_s = 2s/(8n - s)$ and $2\tau_m - \tau_s = 2(2n - s)/(8n - s)$. Using the expression for τ_m given above we have $\tau_s = 8\tau_m - 2$ and $2\tau_m - \tau_s = 2 - 6\tau_m$, generally. It is seen that τ_s corresponds to the lower sideband of τ_m in Fig. 1 and that $2\tau_m - \tau_s$ corresponds to the upper sideband.

The spin-slip structures with an odd ratio of quartets to triplets ($\cdot 1, \cdot 3, \cdot 5$) each possess a small net magnetic moment parallel to the *c* axis. These ferromagnetic states exist over the temperature ranges 51.6–48.5 K, 34.5–31.5 K, and 26.5–23 K which closely agree with the temperatures for which Taylor, Gerstein, and Spedding¹⁴ have observed peaks in the magnetic susceptibility of polycrystalline erbium.

Summarizing the discussion so far, the temperature dependence of erbium's modulation wave vector between

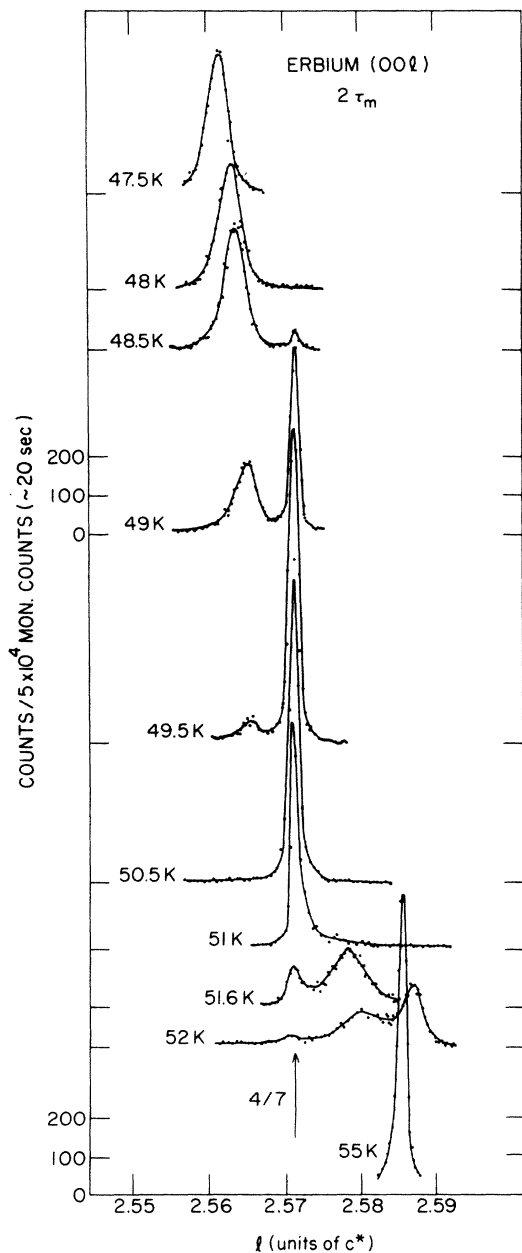


FIG. 3. Temperature dependence of the scattering at $2\tau_m$ near the $\tau_m = \frac{2}{7}$ transition. The peak at $2\tau_m = \frac{4}{7}$ is resolution limited. The solid lines are drawn to guide the eye.

TABLE I. Commensurate *c*-axis spin-slip structures. The \cdot represents a triplet and the integer gives the number of quartets. Also shown are the observed wave vectors of the fundamental magnetic reflection and of the associated lattice modulations.

Commensurate <i>c</i> -axis spin-slip structures				
τ_m	Structure	τ_s	$2\tau_m - \tau_s$	$2\tau_m$
$\frac{2}{7}$	$\cdot 1$	$\frac{2}{7}$	$\frac{2}{7}$	$\frac{4}{7}$
$\frac{3}{11}$	$\cdot 2 \cdot 2$	$\frac{2}{11}$	$\frac{4}{11}$	$\frac{6}{11}$
$\frac{4}{15}$	$\cdot 3$	$\frac{2}{15}$	$\frac{6}{15}$	$\frac{8}{15}$
$\frac{5}{19}$	$\cdot 4 \cdot 4$	$\frac{2}{19}$	$\frac{8}{19}$	$\frac{10}{19}$
$\frac{6}{23}$	$\cdot 5$	$\frac{2}{23}$	$\frac{10}{23}$	$\frac{12}{23}$
$\frac{1}{4}$	2		$\frac{1}{2}$	$\frac{1}{2}$
$\frac{5}{21}$				$\frac{10}{21}$

52 and 18 K exhibits a sequence of commensurate states separated by incommensurate states with characteristically broader diffraction peaks. The description of the commensurate states involves integer ratios of quartets to triplets. Lock-in transitions to higher-order commensurate states, defined as those in which this ratio is a noninteger rational number, were not observed. Instead, the incommensurate diffraction peaks were broadened and indicative of disordered or chaotic states. We note that the lock-in transitions occur in the temperature range where scattering at τ_s and at $2\tau_m - \tau_s$ is observed, suggesting that these lattice modulations help stabilize the commensurate phases. In contrast, the incommensurate states observed above 52 K have resolution limited line widths and no lock-in transitions occur.

To account for the wave vectors observed in the data above 18 K it has not been necessary to consider a spin-slip description of the basal in-plane order.^{4-7,15} We note, however, that the additional charge scattering at τ_s and at $2\tau_m - \tau_s$ is not observed before the basal plane component first appears at 52 K.⁵ It is possible that the local charge distortion arising from the tilt of the electronic quadrupole distribution may enhance the c -axis lattice modulation.

At lower temperatures the observed lattice modulation is further enhanced, and for the ferromagnetic phases $\cdot 3$ and $\cdot 5$ additional allowed scattering appears at the fundamental τ_m , as well as at other odd harmonics. Below 18 K neutron scattering studies⁵ have established the existence of a ferromagnetic component along the c axis in addition to a spiral modulation in the basal plane with $\tau_m = \frac{5}{21}$. A basal plane spin-slip description of the $\frac{5}{21}$ modulation has a sub-period of seven atomic layers suggesting additional scattering at $\frac{2}{7}$ as observed in the x-ray experiments.

We have benefitted from discussions with Per Bak and Jens Jensen. This work was partially carried out at the Stanford Synchrotron Radiation Laboratory which is supported by the U.S. Department of Energy, Office of Basic Energy Science. Work performed in the Brookhaven Physics Department was supported by the Division of Materials Research, U.S. Department of Energy, under Contract No. DE-AC02-76CH00016. The National Synchrotron Light Source is supported by the Divisions of Material Sciences and Chemical Science under Contract No. DE-AC02-76CH00016.

*Permanent address: Riso National Laboratory, Copenhagen, Denmark.

¹See, for example, *Handbook of the Physics and Chemistry of Rare Earth*, edited by K. A. Gschneidner, Jr. and L. R. Eyring (North-Holland, Amsterdam, 1978), Vol. 1.

²D. Gibbs, D. E. Moncton, K. L. D'Amico, J. Bohr, and B. H. Grier, *Phys. Rev. Lett.* **55**, 234 (1985).

³J. Bohr, D. Gibbs, D. E. Moncton, and K. L. D'Amico, in *Proceedings of the Sixteenth International Conference on Thermodynamics and Statistical Mechanics (STATPHYS-16)* [Physica A (to be published)].

⁴J. W. Cable, E. O. Wollan, W. C. Koehler, and M. K. Wilkinson, *Phys. Rev.* **140**, A1896 (1965).

⁵M. Habenschuss, C. Stassis, S. K. Sinha, H. W. Deckman, and F. H. Spedding, *Phys. Rev. B* **10**, 1020 (1974).

⁶M. Atoji, *Solid State Commun.* **14**, 1047 (1974).

⁷J. Jensen, *J. Phys. F* **6**, 1145 (1976).

⁸P. Bak and J. Von Boehm, *Phys. Rev. B* **21**, 5297 (1980).

⁹D. T. Keating, *Phys. Rev.* **178**, 732 (1969).

¹⁰See, e.g., Y. Tsunoda, M. Mori, N. Kunitomi, Y. Teraoka, and J. Kanomori, *Solid State Commun.* **14**, 287 (1974); R. Pynn, W. Press, S. M. Shapiro, and S. A. Werner, *Phys. Rev. B* **13**, 295 (1976).

¹¹D. E. Moncton, D. Gibbs, and J. Bohr, *Nucl. Instrum. Methods Phys. Res. Sec. A* **26**, 839 (1986).

¹²Similar results have been observed in a neutron diffraction study of CeSb by B. Lebeck, C. Broholm, K. Clausen, and O. Vogt, *J. Magn. Magn. Mater.* **54-57**, 505 (1986).

¹³In general the slightly aspherical form factor of the atoms may give rise to an additional scattering component at $2\tau_m$. These effects have been studied in holmium in Ref. 9.

¹⁴See data of W. A. Taylor, B. C. Gerstein, and F. H. Spedding as presented in an article by K. A. McEwen in Ref. 1, p. 428.

¹⁵H. Miwa and K. Yosida, *Prog. Theor. Phys.* **26**, 693 (1961); T. Nagamiya, in *Solid State Physics*, edited by F. Seitz and D. Turnbull (Academic, New York, 1967), Vol. 20, p. 305.